

Dynamic UE clustering for distributed MIMO cooperative transmission

Yuta Seki^{1a)}, Tomoyuki Saito¹, Fumiyuki Adachi¹

¹ Research Organization of Electrical Communication, Tohoku University,
2-1-1 Katahira, Aoba-ku, Sendai, Miyagi 980-8577, Japan

a) seki.yuta@riec.tohoku.ac.jp

Abstract:

Multi-user multiple-input multiple-output (MU-MIMO) using a large number of spatially distributed antennas (DAs) is a promising technique to achieve high link capacity uniformly over a macro-cell area. To reduce the computational complexity of MU-MIMO processing, the UE clustering can be used. However, this produces the inter-cluster interference (ICI) and degrades the link capacity of a user equipment (UE) especially near the cluster boundary. In this paper, to solve the ICI problem, we propose a dynamic UE clustering in which UEs in a macro-cell area are grouped into non-overlapped UE cluster-sets and they are activated in a time-division manner. We evaluate, by computer simulation, the UE link capacity of OFDM downlink achievable by the use of the proposed dynamic UE clustering.

Keywords: Distributed antenna, MU-MIMO, dynamic UE clustering

Classification: Wireless Communication Technologies

References

- [1] ARIB 2020 and Beyond Ad Hoc Group, “Mobile communications system for 2020 and beyond”, White paper, Oct. 2014.
- [2] F. Adachi, A. Boonkajay, Y. Seki, T. Saito, S. Kumagai, and H. Miyazaki, “Cooperative distributed antenna transmission for 5G mobile communications network,” *IEICE Trans. Commun.*, Vol.E100-B, No.8, pp. 1190-1204, Aug. 2017.
- [3] K. Li, R. R. Sharan, Y. Chen, T. Goldstein, J. R. Cavallaro, and C. Studer, “Decentralized baseband processing for massive MU-MIMO systems,” *IEEE J. Emerging Sel. Topics Circuits Syst.*, Vol. 7, No. 4, pp. 491-507, Dec. 2017.
- [4] Yuta Seki, Tomoyuki Saito, and Fumiyuki Adachi, “A Study on Dynamic Antenna Clustering for Distributed MIMO Cooperative transmission using Multi-user MMSE-SVD,” *WPMC 2018*, 25-28 Nov. 2018.
- [5] A. Goldsmith, *Wireless Communication*, Cambridge University Press, 2005.
- [6] D. Tse and P. Viswanath, *Fundamentals of wireless communication*, Cambridge University Press, 2005.

1 Introduction

In the 5th generation (5G) networks, broader-band data services and higher link capacity than in 4G networks are demanded [1]. However, with limited bandwidth and transmit power, the presence of path loss, shadowing loss, and frequency-selective fading makes it quite difficult to achieve high link capacity uniformly over the macro-cell area. As a promising solution, the authors have been studying a MU-MIMO using a large number of spatially distributed DAs over a macro-cell area. However, MU-MIMO using a large number of antennas requires prohibitively high computational complexity [3].

Static UE clustering, in which UEs in a macro-cell area is divided into a number of fixed clusters, can significantly reduce the computational complexity by performing MU-MIMO processing in each cluster independently [4]. However, using the same radio resource in every cluster produces the ICI and reduces the achievable link capacity of a UE near the cluster boundary. In our previous study, we proposed cluster pattern switching which changes periodically the cluster boundary so as to avoid UEs from always falling into the cluster-edge [4]. In this paper, we propose a new dynamic UE clustering, in which spatially non-overlapped UE cluster-sets are constructed in a macro-cell area and they are activated in a time division manner. We evaluate, by computer simulation, the UE link capacities of OFDM downlink achievable with the static UE clustering, the UE cluster switching, and our proposed dynamic UE clustering.

2 Three UE clustering methods

Fig. 1 shows three UE clustering methods assuming a rectangular macro-cell area consisting of uniformly distributed $N_{\text{macro}}=56$ DAs. Each DA covers the small area with radius of R , and all DAs are connected to a macro-cell base station (MBS). The computational complexity of MU-MIMO using all of N_{macro} DAs in a macro-cell area is prohibitively high. Static UE clustering can reduce the computational complexity by performing MU-MIMO multiplexing in each UE cluster independently. However, this produces the ICI from neighbor clusters and degrades the link capacity of cluster-edge UEs. In this paper, cluster-edge is defined as an area of $1/8$ cluster area near both sides of each UE cluster of the static UE clustering. To solve the ICI problem, we propose the dynamic UE clustering and compare with the static UE clustering and cluster pattern switching.

2.1 Static UE clustering

M UE clusters are constructed in a macro-cell area as in Fig.1 (a), where $M=7$. MBS performs MU-MIMO multiplexing in each cluster independently, and therefore the computational complexity can be significantly reduced. Letting Y_m denote a set of UEs in the m th UE cluster, the number of UEs in a macro-cell area is given by $\sum_{m=0}^{M-1} |Y_m| = U_{\text{macro}}$. In each cluster, MBS assigns U UEs to be spatially multiplexed according to the round-robin (RR) manner in the user-index order ($0 \sim |Y_m|-1$). When $|Y_m| < U$, the number of spatially multiplexing UE is to be $|Y_m|$ in the m th cluster.

2.2 Cluster pattern switching

P different cluster patterns, each consisting of M UE clusters, are constructed as in Fig.1 (b), where $M=7$ and $P=2$. The p th cluster pattern is activated at slot time t as $p = t \bmod P$. Letting $Y_{m,p}$ denote a set of UEs in the m th UE cluster of the p th cluster pattern, $\sum_{m=0}^{M-1} |Y_{m,p}| = U_{\text{macro}}$ for any p . In each cluster, MBS assigns U UEs to be spatially multiplexed according to the RR manner in each cluster. When $|Y_{m,p}| < U$, the number of spatially multiplexing UE is to be $|Y_{m,p}|$. It is expected that all UEs can achieve approximately the same average link capacity.

2.3 Dynamic UE clustering

P UE cluster-sets, each having M spatially non-overlapped UE clusters, are constructed in a macro-cell area as in Fig.1 (c), where $M=7$ and $P=2$. Each UE cluster-set is activated in a time division manner. The p th UE cluster-set is activated at slot time t as $p = t \bmod P$, similar to the cluster pattern switching. Differently from the cluster pattern switching, the dynamic UE clustering improves the link capacity of cluster-edge UEs (associated with the static UE clustering) by increasing the co-channel distance using the same radio resource at the same time.

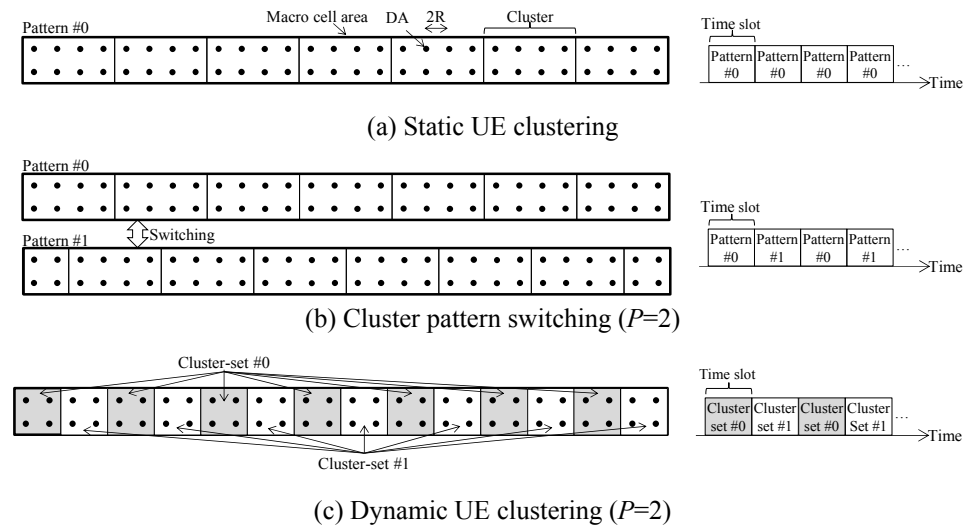


Fig.1. Three UE clustering methods

3 Monte-Carlo computer simulation

3.1 Simulation setting

The UE link capacity is evaluated assuming the rectangular macro-cell. $U_{\text{macro}}=56$ UEs, each equipped $N_{\text{ue}}=2$ antennas, are randomly located in the macro-cell area. $M=7$ clusters for the static UE clustering and $M=7$ and $P=2$ for both the cluster pattern switching and the dynamic UE clustering are considered as in Fig. 1. In each cluster, the MBS assigns $U=2$ UEs according to RR manner with the scheduling period $T_{\text{scheduling}}=56$. The number of data streams per UE is assumed to be $N_{\text{strm}}=2$. For each assigned UE, $N_{\text{mbs}}=4$ DAs are selected beyond the cluster boundary in a descending order of the sum of pathloss and shadowing loss between

each DA and assigned UE. The MU-MIMO processing called MMSE-SVD [2] is applied to multiplex 2 UEs in each cluster. The MBS's MMSE transmit filter matrix and the u th UE's eigenmode receive filter matrix for the k th subcarrier ($k=0\sim N_c-1$) are given as [2]

$$\begin{cases} \mathbf{W}_{\text{mmse}}(k) = [\mathbf{W}_{\text{mmse},0}(k), \dots, \mathbf{W}_{\text{mmse},u}(k), \dots, \mathbf{W}_{\text{mmse},U-1}(k)] \\ \quad = (\mathbf{U}^H(k)\mathbf{H}(k))^H \left((\mathbf{U}^H(k)\mathbf{H}(k))(\mathbf{U}^H(k)\mathbf{H}(k))^H + \left(\frac{E_s}{N_0}\right)^{-1} \frac{N_{\text{ue}}}{N_{\text{strm}}} \mathbf{I}_{U \cdot N_{\text{strm}}} \right)^{-1} \mathbf{P}^{1/2}(k), \quad (1) \\ \mathbf{W}_{\text{svd},u}(k) = \mathbf{U}_u^H(k) \end{cases}$$

where E_s is symbol energy and N_0 is the single-sided power spectrum density of the additive white Gaussian noise (AWGN), $\mathbf{H}(k) = [\mathbf{H}_0^T(k), \dots, \mathbf{H}_{U-1}^T(k)]^T$ is the $(U \cdot N_{\text{ue}}) \times N_{\text{mbs}}$ downlink MU-MIMO channel matrix. $\mathbf{U}(k) = \text{diag}[\mathbf{U}_0(k), \dots, \mathbf{U}_{U-1}(k)]$ with $\mathbf{U}_u(k)$ is a unitary matrix obtained by applying SVD [5] to $\mathbf{H}_u(k)$, and $\mathbf{P}(k) = \text{diag}[\mathbf{P}_0(k), \dots, \mathbf{P}_{U-1}(k)]$ with $\mathbf{P}_u(k)$ of size $N_{\text{strm}} \times N_{\text{strm}}$ represents the water filling based power allocation [6] across eigenmodes and subcarriers. The MMSE transmit filter and the eigenmode receive filter are used for suppressing both the inter-antenna interference and the inter-user interference and for suppressing the inter-antenna interference, respectively.

The wireless channel is characterized by distance-dependent path loss, log-normally distributed shadowing loss, and multipath fading. In this paper, the path loss exponent $\alpha=3.5$ and the shadowing loss standard deviation $\eta_{u,n_{\text{mbs}}} = 7$ (dB) are assumed. The type of fading is assumed to be the Nakagami-Rice with the dominant path-to-scattered path power ratio $K=10$ (dB) if the distance $d_{u,n_{\text{mbs}}}$ between the u th UE and the n_{mbs} th DA is equal to or smaller than R , and is assumed to be the Rayleigh (i.e., $K=0$) if $d_{u,n_{\text{mbs}}}$ is larger than R . The transfer function $H_u(k; n_{\text{ue}}, n_{\text{mbs}})$ between the n_{ue} th antenna of the u th UE and the n_{mbs} th DA can be represented as

$$H_u(k; n_{\text{ue}}, n_{\text{mbs}}) = \sqrt{d_{u,n_{\text{mbs}}}^{-\alpha} 10^{\frac{\eta_{u,n_{\text{mbs}}}}{10}}} \left\{ \begin{aligned} & \sqrt{\frac{K}{K+1}} \exp(j\theta_{u,n_{\text{ue}},n_{\text{mbs}}}) \exp\left(-j \frac{2\pi k \tau_{u,n_{\text{ue}},n_{\text{mbs}}}(0)}{N_c}\right) \\ & + \sqrt{\frac{1}{K+1}} \sum_{l=0}^{L-1} \xi_{u,n_{\text{ue}},n_{\text{mbs}}}(l) \exp\left(-j \frac{2\pi k \tau_{u,n_{\text{ue}},n_{\text{mbs}}}(l)}{N_c}\right) \end{aligned} \right\}, \quad (2)$$

where L denotes the number of resolvable paths, $\theta_{u,n_{\text{ue}},n_{\text{mbs}}}$ is the phase of dominant path and is assumed to be distributed uniformly, $\xi_{u,n_{\text{ue}},n_{\text{mbs}}}(l)$ and $\tau_{u,n_{\text{ue}},n_{\text{mbs}}}(l) = l$ are respectively the complex-valued path gain and the sample-spaced time delay of the l th path with $E[\sum_{l=0}^{L-1} |\xi_{u,n_{\text{ue}},n_{\text{mbs}}}(l)|^2] = 1$ for all u, n_{ue} , and n_{mbs} , and $H_u(k; n_{\text{ue}}, n_{\text{mbs}})$ is the $(u \cdot N_{\text{ue}} + n_{\text{ue}}, n_{\text{mbs}})$ th element of MU-MIMO channel matrix $\mathbf{H}(k)$.

OFDM downlink capacity \bar{C}_u (bps/Hz/ $T_{\text{scheduling}}$) of the u th UE is computed using the Shannon capacity formula as

$$\bar{C}_u = \frac{1}{T_{\text{scheduling}}} \sum_{t=0}^{T_{\text{scheduling}}} \sum_{n_{\text{strm}}=0}^{N_{\text{strm}}-1} \frac{1}{N_c} \sum_{k=0}^{N_c-1} \log_2(1 + \gamma_u(t; k; n_{\text{strm}})), \quad (3)$$

where $\gamma_u(t; k; n_{\text{strm}})$ denotes the instantaneous signal-to-interference plus noise ratio (SINR) after the eigenmode reception at u th UE.

3.2 Simulation result

Fig. 2 plots the cumulative distribution function (CDF) of the UE link capacity of cluster-edge UEs (associated with the static UE clustering) and that of UEs all over macro-cell for $N_c=1024$, the normalized transmit $E_s/N_0=30$ (dB), and $L=16$. From Fig. 2 (a), it can be seen that overall the dynamic UE clustering provides highest link capacity than other two clustering methods. The cluster pattern switching provides only a slightly superior capacity in a very low capacity region, but it provides the link capacity close to that of the static UE clustering in a high capacity region. This is because that cluster pattern switching only averages the link capacity in a strong and a weak ICI conditions while the dynamic UE clustering reduced the ICI by increasing the distance between adjacent co-channel clusters using the same radio resource at the same time. The dynamic UE clustering can improve the UE link capacity at 10% (90%) CDF of cluster-edge UEs by about 2.2 (1.1) times compared with the static UE clustering. A similar conclusion can be seen in Fig. 2 (b). Overall the dynamic UE clustering can provides highest link capacity than other two clustering methods while the cluster pattern switching provides clearly a worse capacity than the static UE clustering in a high capacity region.

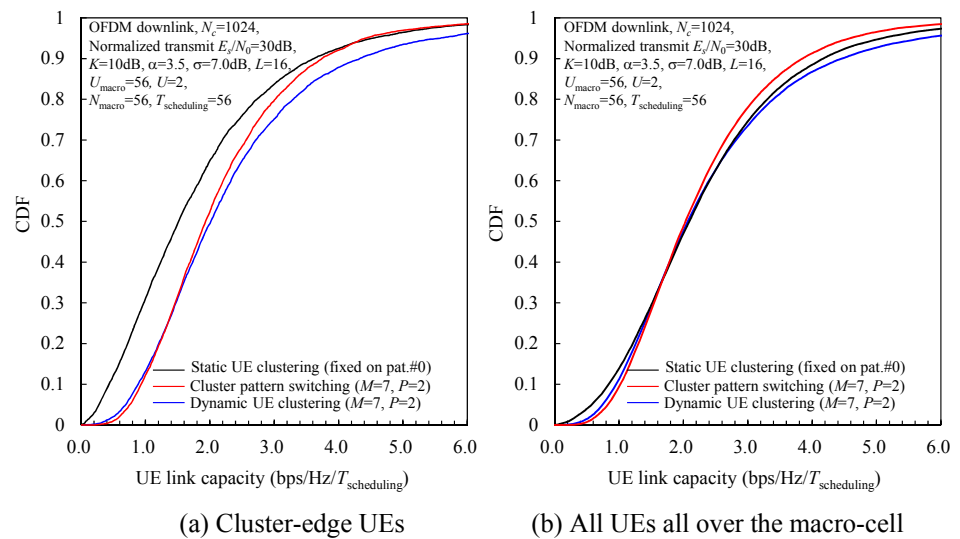


Fig.2. UE Link capacity

4 Conclusion

In this paper, we evaluated the effect of our proposed dynamic UE clustering on the UE link capacity by computer simulation. Overall, the dynamic UE clustering provides highest link capacity than other two clustering methods; it improves the UE link capacity at 10% (90%) CDF of cluster-edge UEs (associated with the static UE clustering) by about 2.2 (1.1) times compared with the static UE clustering. In this paper, uniformly distributed UE locations was considered. However, in practical situations, the UE distribution is not uniform. The adaptive clustering considering the UE distribution is left as an interesting future study item.

Acknowledgments

The results presented in this paper have been achieved by “The research and development project for realization of the fifth-generation mobile communications system,” commissioned to Tohoku University by The Ministry of Internal Affairs and Communications (MIC), Japan.